arXiv:0810.1757v1 [cond-mat.mes-hall] 10 Oct 2008

Scenario for Fractional Quantum Hall Effect in Bulk Isotropic Materials

F. J. Burnell[1], B. Andrei Bernevig[1,2] and D. P. Arovas[3]
[1] *Department of Physics, Princeton University, Princeton, NJ 08544*
[2] *Princeton Center for Theoretical Physics, Princeton, NJ 08544 and*
[3] *Physics Department 0319, University of California at San Diego, La Jolla, CA 92093*

(Dated: October 10, 2008)

We investigate the possibility of a strongly correlated Fractional Quantum Hall (FQH) state in bulk three dimensional isotropic (not layered) materials. We find that a FQH state can exist at low densities only if it is accompanied by a staging transition in which the electrons re-organize themselves in layers, perpendicular to the magnetic field, at distances of order the magnetic length apart. The Hartree energy associated to the staging transition is off-set by the correlation Fock energy of the 3D FQH state. We obtain the phase diagram of bulk electrons in a magnetic field subject to Coulomb interactions as a function of carrier density and lattice constant. At very low densities, the 3D FQH state exhibits a transition to a 3D Wigner crystal state stabilized by phonon correlations.

PACS numbers: 73.43.f, 11.25.Hf

The Quantum Hall effect is intimately linked to the low-dimensionality of the sample and the fact that the magnetic field quenches the kinetic energy of the electron liquid in 2 dimensions (2D). The Quantum Hall effect has also been observed in 3 dimensions (3D) in the Bechgaard salts [1, 2] but only at integer filling factors and only in layered samples. The 3D Quantum Hall states can be explained as a series of 2D states, weakly coupled so that the band-width in the z-direction be smaller than the 2D Landau gap. So far, 3D FQH states have not been observed, even in layered samples, due to their low electron mobility and small many-body gap.

Recent experimental interest in graphene, graphite and Bismuth has focused on the Dirac nature of carriers and on the Integer Quantum Hall (IQH) effect. The Dirac dispersion in these materials gives electrons large mean-free paths and large Landau gaps. As a result, large IQH plateaus are observed, even at room temperature. A 3D IQH effect has been predicted in graphite [3]. Band structure considerations suggest that, at sufficiently strong magnetic field, the $n = 0$ and $n = 1$ Landau levels of graphite are gapped and a single 3D IQHE plateau exists. The layered structure of graphite is essential to the existence of the 3D IQH. Recent experiments in Bismuth suggest the possibility of a 3D bulk strongly correlated electron state in the fractional filling regime [4]. The experiment reports quasi-plateaus in ρ_{xy} at fields which are integer times larger than the field required to drive the system in the quantum limit.

These results are unexpected since Bismuth, unlike Graphite, is an isotropic material. There are only two known scenarios for the existence of a Quantum Hall effect in 3D: it can be either a band-structure effect, such as in graphite, or an interaction effect, where a $2k_F$ instability opens a gap at the one dimensional Fermi level in the direction of the magnetic field. The Fermi level is then pinned in the many-body gap and the system exhibits a Quantum Hall effect. However, by construction, both these scenarios lead to an integer, and not fractional state. While it is easy to generalize the Laughlin [5] and Halperin [6] states to a 3D FQH state [7, 8] with correlations between layers, they were never found to be the variational ground-states in an isotropic material. Contrarily, it was found [7] that the magnetoplasmon gap closes and a phase-transition to a crystal state occurs whenever the distance between the layers is roughly smaller than half the magnetic length.

Previous work on quantum well bi-layer and multilayer systems suggests several possible electronic arrangements for a 3D material in a magnetic field: MacDonald and coauthors [9] considered the energetics of 3D Halperin states, which are adaptations of the Laughlin wave functions to ensure that electrons in adjacent layers maximize their separations. At very small inter-layer separations, they found these states crystalize due to a collapse of the magnetoroton gap. MacDonald [7] also established that in multilayers, in the Hartree Fock approximation, the gain in exchange energy from distributing electrons unequally between the layers can exceed the electrostatic cost of increased inter-layer Coulomb energy leading to a *staging transition*. Ref. [10] proposed a third type of candidate state, the spontaneous inter-layer coherent miniband state, consisting of a combination of lowest Landau level (LLL) states in each layer which forms a band in k_z. However, no state exhibiting a 3D FQH effect has been found as the ground-state of an isotropic material in $\vec{B}$ field.

In this paper, we revisit these issues and try to address the question of whether a FQH effect could exist in the 3D compound. We propose a new variational ground-state, a correlated 3D FQH-staged state in an isotropic material. We compare four different potential ground states for materials in $\vec{B}$ field in the ultra-quantum limit with strong Coulomb interactions and find that 3D FQH ground-states do not occur in isotropic materials unless they are accompanied, at very low densities, by staging transitions similar to the ones observed in graphite intercalation compounds [11] and predicted to occur in multi-quantum-well systems by MacDonald [7]. In the parameter range relevant to both graphite and Bismuth, we obtain the phase diagram as a function of the electron filling fraction, the ratio of inter-layer separation to magnetic length, and the magnitude of the c-axis hopping. At high carrier density and zero c-axis hopping, a (staged) integer quantum Hall liquid is energetically favorable. As the filling in occupied layers decreases below $\nu = 1$, liquid states with correlations between layers can develop, and become energetically favored because of their decreased inter-planar Coulomb energy. At extremely low densities, staged crystal states tend to be energetically favored. A SILC miniband state becomes favored over the staged integer liquids, but not their fractional counterparts, at the c-axis hopping relevant to graphite. Thus we find a parameter regime in which fractionally filled, staged quantum Hall liquid states are the expected ground states of the layered system.

Let us consider an isotropic material subject to a magnetic field parallel to one of its crystallographic axes. The magnetic field quenches the kinetic energy of electrons in lattice planes (layers) perpendicular to the magnetic field. A plausible scenario, borrowed from MacDonald's work on staged states in multiple quantum wells [7] is that the relatively small inter-layer separations in isotropic materials favor staged states which consist of n layers of electron gas of density $\overline{\sigma}_e - \delta\sigma$, and one layer of density $\overline{\sigma}_e + n\delta\sigma$, where $\overline{\sigma}_e$ is the initial electron density per layer, and $\delta\sigma$ is the staging density. For crystalline states, staging increases the distance between electrons which lie directly above one another, decreasing the crystal's Coulomb energy at small inter-layer separations; for liquid states staging becomes advantageous when the gain in Fock energy by increasing the electron density in the filled layers outweighs the Hartree cost of distributing charge unevenly between the layers. Thus as the separation between layers decreases, staged states become increasingly energetically favorable.

We calculate the staging Hartree energy as described in [7]. We model the system as a stack of planes, each of uniform charge density σ_i, where $\sigma_i = -n\delta\sigma$ if $i|(n+1)$ and $\delta\sigma$ otherwise. This charge density is comprised of an immobile positive background (ionic) charge density $\overline{\sigma}_e$ in each plane, and a staged electronic charge density $-\overline{\sigma}_e + \sigma_i$. n is called the *staging number.* The 3-d charge density is conveniently described in Fourier space as a sum of Kroeneker δ terms

$$\begin{aligned}\rho(q_z) &= \rho_1(q_z) + \rho_2(q_z) \\ \rho_1(q_z) &= \delta\sigma\frac{V}{d}\sum_j \delta(q_z, 2\pi j/d) \\ \rho_2(q_z) &= -\delta\sigma\frac{V}{d}\sum_j \delta(q_z, 2\pi j/(n+1)d) \qquad (1)\end{aligned}$$

where V is the total sample volume, and d is the lattice constant in the direction of the magnetic field. This charge density configuration has a Hartree energy $E_s = \frac{e^2}{\epsilon V}\sum_{q_z}\frac{2\pi}{q_z^2}|\rho(q_z)|^2$, or:

$$E_s = \frac{e^2}{\epsilon l}\frac{(\delta\nu)^2}{\nu_0}\frac{d}{12l}(n^2+2n) \qquad (2)$$

where $\nu_0 \equiv 2\pi l^2\overline{\sigma}_e$, and $\delta\nu = 2\pi l^2\delta\sigma$ is the electronic filling staged from each layer. One could also consider multiply staged states, in which three or more different staging numbers n exist. However, we numerically found that the states of lowest energy are those with charge distributions of the form in Eqn. (1), described by a single staging number.

The first class of candidate states that we consider are the staged liquid states. The simplest such staged liquids consist of n layers depleted of electrons, and one layer of electronic charge density $\overline{\sigma}_e + n\delta\sigma$ (which we will call the occupied layer) in a quantum Hall liquid state. The total energy of a staged liquid state is then:

$$E = \frac{n}{n+1}E_l(\nu_0 - \delta\nu) + \frac{1}{n+1}E_l(\nu_0 + n\delta\nu) + E_s \qquad (3)$$

where n is the staging number, $E_l(\nu)$ is the energy of the liquid at filling ν, E_s is the Hartree energy given by (2), ν_0 is the mean filling factor, and $0 \leq \delta\nu \leq \nu_0$ is the amount of charge staged out of each layer.

As Laughlin states have good in-plane correlation energies, we consider first the case where the occupied layers are in a Laughlin state. We will refer to Laughlin states at filling fraction $1/m$ in the occupied layers as $(0, m, 0)$ states. Since the filling fraction in these layers is then fixed at a value of $\nu = 1/m$ for some odd integer m, the quantities ν, ν_0 and n are related by $n + 1 = \frac{\nu}{\nu_0}$. Using (3), the optimal staged liquid state for a given ν_0 and d/l can be found by optimizing over $\delta\nu$ and n. We find that optimal states in the regimes of interest are fully staged ($\delta\nu = \nu_0$), so that the first term of the right-hand side of (3) vanishes.

At small d/l, the simple uncorrelated liquid state described above gives way to liquids with inter-layer correlations [9], which we call Halperin liquid states. These states have wave functions of the form

$$\psi = \prod_{k;i,j}(z_i^{(k)} - z_j^{(k-1)})^{m_1}(z_i^{(k)} - z_j^{(k+1)})^{m_1}\prod_{i<j}(z_i^{(k)} - z_j^{(k)})^{m_2} \qquad (4)$$

where k indexes the layer, and i, j index particles within a layer. We refer to states of the form (4) as (m_1, m_2, m_1) states. Fig. [1] shows the energies for several of these states as a function of inter-layer separation and density, calculated using Monte Carlo techniques (see Appendix).

When d/l is very small, one can imagine a low energy ground state of staged Halperin liquid states, with n layers completely depleted of electronic charge for every occupied layer at filling $\nu = 1/(2m_1 + m_2)$. In the

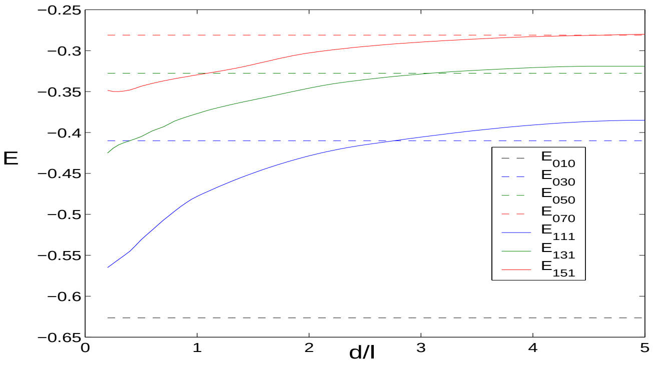

FIG. 1: Energies of unstaged Laughlin (dashed lines) and Halperin (solid lines) liquid states as a function of inter-layer separation over magnetic length (d/l). All energies are reported as energies per electron, in units of $\frac{e^2}{\epsilon l}$, where l is the magnetic length. At large separation the energy increases with d/l as the correlations in Eqn. (4) do not optimally minimize the intra-planar Coulomb interactions and their energy grows (see text). The minimum energy occurs when correlations effectively separate electrons from both their in-plane and out-of-plane neighbors.

layered system with a given mean filling per layer ν_0, the staging number is fixed by $n+1 = \frac{1}{\nu_0(2m_1+m_2)}$. This in turn fixes the separation $(n+1)d$ between occupied layers, and the energy of such a state is

$$E = E_l((n+1)d) + E_s(d, n, \nu) \tag{5}$$

where $E_l((n+1)d)$ is the Coulomb energy of the state (4) at inter-layer separation $(n+1)d$, extrapolated from the Monte Carlo results of fig. 1, and E_s is the Hartree staging term. Fig. 1 shows an important property of the energies as a function of d/l. The wave function (4) contains correlations which separate electrons in adjacent layers, at the expense of decreasing their average separation in a given layer. Since these correlations do not depend on d/l (the out of plane correlations in Eqn. (4) depend on $z_i^{(k)} - z_j^{(k-1)}$, i.e. only on the in-plane distance between particles in different layers), as d/l increases the energy of the Halperin states also tends to increase. The inter-planar Coulomb interaction becomes weaker, so that the energetic gain from inter-layer correlations decreases, while the energetic cost of decreased separation in-plane relative to the Laughlin state of the same filling remains constant. At large d/l the Laughlin liquid becomes the ground state.

In two dimensions, it is well known that for a low density of carriers, a transition occurs from a FQH state to a triangular lattice Wigner crystal of lattice constant $a = l\left(\frac{\sqrt{3}\pi}{\nu}\right)^{1/2}$. The Wigner crystal is energetically favored over the FQH liquid state at fillings $\nu < 1/7$ [12]. In multi-layer systems at small d ($d/l < 0.9\sqrt{\frac{2\pi}{\nu}}$), inter-layer repulsions favor an in-plane lattice that is square as this permits larger separations between sites in neighboring planes [9]. As d decreases, multiple phase transitions between different stackings of squares in the vertical direction occur; reference [9] identifies states in which electrons at the same in-plane co-ordinates are separated by $M = 2$, 4 or 5 layers, as well as states with incommensurate stackings. In this work we consider only true crystal states with well-defined spatial periodicity, and will not include structures with incommensurate stackings.

Numerical studies [12] indicate that the total energy of these crystalline states is well approximated by

$$E = E_0\,\nu^{1/2} + E_2\,\nu^{3/2} + E_3\,\nu^{5/2}. \tag{6}$$

Here E_0 is the classical contribution, given by the energy of the Madelung sum, E_2 is the phonon contribution, and E_3 is an extra higher moment contribution calculated by a fit to a numerical evaluation of the Coulomb energy. For the low fillings at which Wigner crystals are expected to occur, the total energy is well approximated by the first two terms.

The classical contribution E_0 can be calculated using the Ewald method, described in detail in [13]. We slightly modify this method to account for the fact that the background charge is localized in the planes. At each value of d, energies were tabulated for a variety of crystal stackings and stagings; the configurations of lowest energy were selected. We estimate E_3 by numerically extrapolating the results of [9] as a function of nd/l to the values of interest here ($(n+1)d/l \approx 0.2$ for most optimally staged crystal states).

We compute the contribution of lattice vibrations E_2 by postulating a Lam-Girvin [12] variational wave function of the form

$$\Psi = \exp\left(\frac{1}{4}\sum_{ij}\xi_i\,B_{ij}\,\xi_j\right)\prod_j \phi_{\vec{R}_j}(\vec{r}_j) \tag{7}$$

Here $\vec{R}_j = (X_j, Y_j)$ is the position of the lattice site, $\xi_j \equiv (x_j - X_j) + i(y_j - Y_j)$ is the deviation of the particle's position from this site in two-dimensional complexified coordinates, and $\phi_{\vec{R}}(\vec{r})$ are the lowest Landau level coherent states,

$$\phi_{\vec{R}}(\vec{r}) = \frac{1}{\sqrt{2\pi l^2}}\, e^{-(\vec{r}-\vec{R})^2/4l^2}\, e^{i\hat{z}\cdot\vec{r}\times\vec{R}/2l^2} \tag{8}$$

The correlation matrix B is a variational parameter; minimizing the variational energy gives

$$B_{\vec{k}} = \frac{\omega_L(\vec{k}) - \omega_T(\vec{k})}{\omega_L(\vec{k})\,\omega_T(\vec{k})} e^{i\theta_{\vec{k}}}$$

$$E_2 = \frac{m_e^* l^2}{4}\sum_{\vec{k}}\left(\omega_L(\vec{k}) + \omega_T(\vec{k})\right)^2 \tag{9}$$

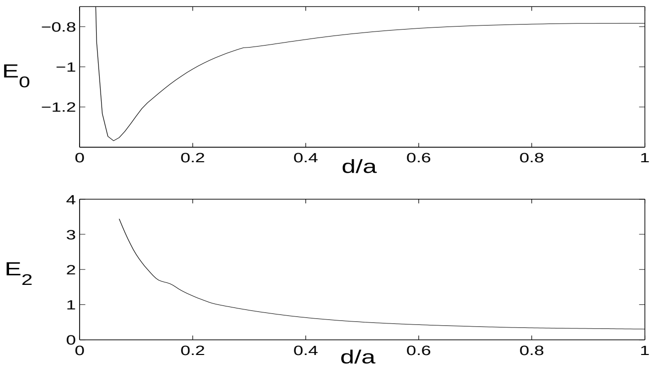

FIG. 2: Calculated energies (per electron) of the unstaged crystalline states, as a function of d/a where a is the crystal lattice constant. Energies are shown in units of $\frac{e^2}{\epsilon l}$. Top: Coulomb sum contribution (E_0). As d/a decreases several phase transitions occur to crystal stacking patterns with a larger unit cell in the z direction, consistent with the findings of [9]. Bottom: Phonon contribution (E_2) for the crystal states of lowest E_0. As d/a decreases the mean inter-electron distance decreases and E_2 grows.

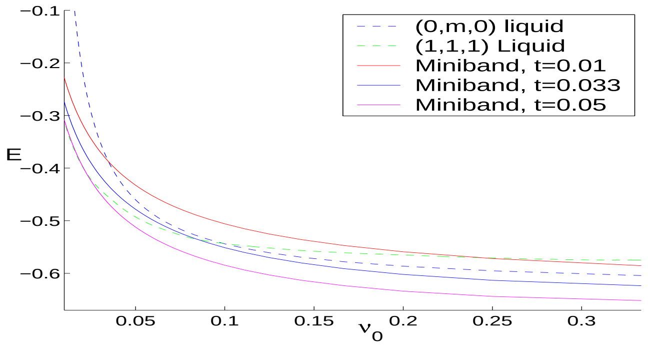

FIG. 3: A comparison of the energies of the $(0,1,0)$ and $(1,1,1)$ staged liquids with those of SILC miniband states as a function of mean filling for $d/l = 0.1$. Energies and $t_\perp$ are shown in units of $\frac{e^2}{\epsilon l}$. At the physical value $t_\perp = 0.033 \cdot e^2/\epsilon l$ the SILC miniband state is energetically favored at high densities, and has lower energy than the staged integer-filled liquid state. The ν_0 dependence of the liquid energies can be understood from fig. 1 by noting that at fixed d/l and occupied filling ν, $nd/l = \nu d/l\nu_0$).

where ω_L and ω_T are the longitudinal and transverse phonon frequencies, respectively, and E is the energy of the phonon modes. The phonon frequencies are calculated using the method of [14]. For multiple-site unit cells, we fix B_k as a single function independent of site indices within the unit cell. In this case the energy is given by (9), with ω_T, ω_L replaced by the square roots of the eigenvalues of the 2×2 matrix formed by averaging the second order correction to the Coulomb potential over all sites in the unit cell.

Fig. 2 shows the energies E_0 and E_2 of the crystalline states over a range of inter-layer separations. At very small d/a, the dominant interaction for a M-layer crystal stacking is between an electron and its translates M layers above and below; the associated energy increases roughly as $\frac{1}{Md}$. To avoid this cost, the crystal undergoes several transitions to stackings of higher M over the range of inter-layer separations shown in fig. 2 [9]; at sufficiently small d/a even the $M = 5$ stacking does not adequately separate charges from their closest vertical neighbors and the energy grows rapidly. Though we computed the energy of all three crystal structures (2- 4- and 5- layer crystal stackings) at each value of d/a, only the lowest of these energies is shown in the fig. 2.

At the very small values of d/l found in graphite and bismuth, none of these crystal structures represent a stable ground state. We therefore allow for Wigner crystals with staged charge densities, requiring that charge depleted layers be completely emptied of electrons ($\delta\sigma = \overline{\sigma}_e$). The total energy for the staged Wigner crystal is given by

$$E = E_{\text{crys}} + E_s \tag{10}$$

where E_{crys} is given by (6), using the values of E_0 and E_2 shown in fig. 2 at the effective inter-layer separation $(n+1)d$, and E_s is given by (2) with $\delta\nu = \nu_0$. At a given inter-layer separation d and mean filling ν_0, we find the energetically optimal Wigner crystal by choosing the staging number which minimizes (10).

The final candidate state we consider is the Spontaneous Inter-Layer Coherent State (SILC) miniband of Hanna, Díaz-Vélez, and MacDonald [10]. The SILC is given by the Slater determinant state

$$|\psi\rangle = \prod_{q,X} C^\dagger_{q,X}|0\rangle \tag{11}$$

where the creation operator generates the state

$$\begin{aligned} \langle\vec{r}|C^\dagger_{q,X}|0\rangle &= \frac{1}{\sqrt{N_{\text{p}}}} \sum_{j=1}^{N_{\text{p}}} e^{ijqd} \psi_{j,X}(\vec{r}) \qquad (12)\\ \psi_{j,X}(\vec{r}) &= \frac{1}{\sqrt{2\pi l^2}}\, \chi(z - jd)\, e^{iXy/l^2}\, e^{-(x-X)^2/2l^2}\ , \end{aligned}$$

Here, X is the center of the Landau strip, and $\chi(z - jd)$ describes the vertical localization of the electron to the j^{th} plane; N_{p} is the number of planes (layers). The product X is over all states in the lowest Landau level (LLL), but only the lowest energy states in the momentum band are filled: $-\pi\nu/d < q \le \pi\nu/d$.

The energy of the SILC is given by [9]

$$\frac{E_c}{N_e} = \frac{\nu e^2}{\epsilon l} \sum_j \int \frac{d^2 r}{4\pi l^2} e^{-r^2/2l^2} \left(\frac{\sin(\pi j \nu)}{\pi j \nu}\right)^2 - \frac{2 t_\perp \sin(\pi\nu)}{\pi\nu} \tag{13}$$

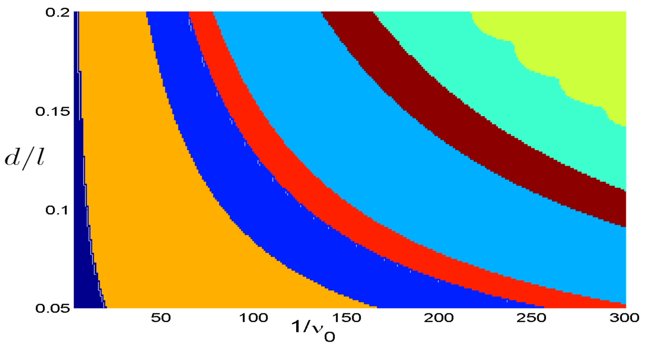

FIG. 4: Approximate phase portrait for graphite in the range $B \approx 30T$. SILC miniband states are navy blue; the Laughlin liquids are colored dark blue ((0,3,0) state), pale blue ((0,5,0) state), and turquoise ((0,7,0) state). The Halperin liquids are colored orange ((1,1,1) state), red ((1,3,1) state), and brown ((1,5,1) state). Crystalline states are shown in green.

where $t_\perp$ is the hopping matrix element in the stacking direction. Fig. 3 compares the energies of the SILC miniband states at $d = 0.1$ for several $t_\perp$ values with the energies of the staged liquid states. The energy of the SILC miniband state depends strongly on the c-axis hopping matrix element $t_\perp$. For $t_\perp = 0.01\frac{e^2}{\epsilon l}$, at the values of d pertinent to graphite the SILC miniband state is never a ground state, as shown in the fig. 3. At intermediate values ($t_\perp = 0.03\frac{e^2}{\epsilon l}$), the SILC miniband state is the ground state for sufficiently high densities. For $t_\perp \geq 0.05\frac{e^2}{\epsilon l}$, the SILC miniband state is the ground state for all densities shown.

We now compare the energies of the three types of states outlined before in a parameter regime experimentally attainable for graphite. We model graphite as a quantum Hall multilayer of graphene sheets. Within each graphene plane, we assume that the magnetic length is sufficiently large that the positive charge of the graphene crystal is well approximated as a uniform surface charge $\overline{\sigma}_e$. Further, we take the inter-plane separation d to be fixed, with a value of approximately $d = 3.4\,\text{Å}$. We consider relatively strong magnetic fields ($B \approx 30\,\text{T}$).

In graphite, at $B = 30\,\text{T}$, the relevant length scales is $l = 47\,\text{Å}$, giving $d/l \approx 0.07$. The c-axis hopping in the LLL, as calculated from the c-axis bandwidth of the LLL [3], is $t_\perp \approx 10\,\text{meV}$ and the Landau gap is given by $E_{\text{gap}} = 30\,\text{meV}$. The energy scale is set by $\frac{e^2}{\epsilon_0 l} = 0.31\,\text{eV}$. We assume that the mean filling fraction can be tuned independently of the magnetic field.

The expected phase portrait for the system is shown in fig. 4. At constant d/l, as the mean filling decreases (in real materials, these would be differently doped samples), the ground state shifts from a SILC miniband state through $(1,1,1)$, $(0,3,0)$, $(1,3,1)$, $(0,5,0)$, $(1,5,1)$, and $(0,7,0)$ liquid states; at sufficiently low ν_0 a phase transition to a staged crystalline state (shown in green) occurs. At physically relevant values of $t_\perp \approx 0.03\frac{e^2}{\epsilon_0 l}$, the SILC miniband state is the ground state only at high densities where integer-filled Laughlin liquids would otherwise occur.

The structure of the phase portrait reflects the competition between Hartree and Fock energy contributions. The Fock energy decreases with increasing density, and thus always favors maximal staging. As ν_0 decreases at fixed d, the Fock energy of staging to a given filling ν remains fixed, while the Hartree energy due to staging increases approximately linearly in $n + 1 = \nu/\nu_0$. Hence a series of transitions to states of lower filling in the occupied layers occurs. Once $\nu < 1/7$, the crystalline states have lowest energy. At fixed ν, a transition occurs between a Halperin state at higher ν_0 (and hence smaller separation nd between occupied layers) and a Laughlin liquid at lower ν_0 (favored at larger nd). The effect of increasing d at fixed ν_0 is similar: it increases the effective cost of staging, and hence favors less filled states; at fixed ν a phase transition between Halperin and Laughlin liquid states occurs.

The crystalline states investigated in this paper have all assumed 'pancake' charge distributions confined to individual lattice planes. However, c-axis hopping will allow the electron charge distribution to spread out in the z-direction. For weak hopping, the crystalline states should be stable throughout much of their phase diagram, but eventually as $t_\perp$ increases, states like the SILC are preferred. In the continuum, one can define a family of variational three-dimensional crystalline states as generalizations of the two-dimensional quantum Wigner crystal of Maki and Zotos [15], writing

$$\Psi = \det\left[\psi_{\vec{R}_i, Z_i}(\vec{r}_j, z_j)\right] , \tag{14}$$

where $\vec{r}_j$ is the electron position projected onto the (x, y) plane, and z is the c-axis coordinate, and where

$$\psi_{\vec{R},Z}(\vec{r}, z) = \phi_{\vec{R}}(\vec{r})\,\varphi(z - Z) \tag{15}$$

is a product of the in-plane lowest Landau level coherent state and a trial single particle wavefunction describing the localization of the electron along the c-axis. An obvious choice for $\varphi(z)$ would be a harmonic oscillator wavefunction with a length scale λ that is a variational parameter, determined by the local curvature of the self-consistent crystalline potential. In this paper, we *underestimate* the stability of our crystalline states; allowing the electrons to delocalize somewhat in the transverse dimension will lower their energy. We will report on calculations based on these states, and their obvious extensions to correlated Wigner crystal states described in Eqn. 7, in a future publication.

We conclude that fractionally filled quantum Hall states cannot occur as stable ground-states in isotropic materials under realistic $\vec{B}$ fields for which the magnetic length is much larger than the c-axis lattice constant unless the density is sufficiently low so that a staged FQH state becomes energetically favorable. At even smaller densities, the FQH staged ground-states give way to a staged 3D Wigner crystal with large unit cells in the direction parallel to the magnetic field.

Acknowledgments – FB and BAB gratefully acknowledge conversations with F. D. M. Haldane and S. L. Sondhi. DPA is grateful to the support and hospitality of the Stanford Institute for Theoretical Physics during the early stages of this work.

Appendix: To use the Monte Carlo method initially used by Laughlin for FQH systems [5] in a layered system, we chose periodic boundary conditions and compute the Coulomb energy of each configuration as a Ewald sum over repeated copies of the fundamental cell. Particle configurations are generated with a probability dictated by the squared wave function; the energy is calculated by averaging the Coulomb potential over a large number of configurations. The fundamental cell is a square in plane of side length $\sqrt{2\pi l^2 N_{\rm 2D}/\nu}$, where $N_{\rm 2D}$ is the total number of particles per layer. These dimensions are chosen to enclose the maximum possible area over which the distribution of electrons in a droplet is essentially uniform, minimizing boundary effects. At each step in the simulation, only particles which are found within the fundamental cell are included in calculating the energy, though particles outside this region may return at a later Monte Carlo step.

The vertical dimensions of the fundamental cell are determined by the minimum number of layers which gives accurate energies. The height of the unit cell $N_{\rm layers}d$ must be at least several times the mean in-layer interparticle spacing; otherwise the computed energy will be artificially high due to particles $N_{\rm layers}+1$ layers apart which lie directly above each other. At very small d this limits the accuracy of the simulations, as extremely large numbers of layers must be used to obtain reasonable values.

[1] L. Balicas, G. Kriza, and F. I. B. Williams, Phys. Rev. Lett. **75**, 2000 (1995).

[2] S. K. McKernan, S. T. Hannahs, U. M. Scheven, G. M. Danner, and P. M. Chaikin, Phys. Rev. Lett **75**, 1630 (1995).

[3] B. A. Bernevig, T. L. Hughes, S. Raghu, and D. P. Arovas, Phys. Rev. Lett **99**, 146804 (2007).

[4] K. Behnia, L. Balicas, and Y. Kopelevich, Science **317**, 1729 (2007).

[5] R.B. Laughlin, Phys. Rev. Lett. **50**, 1395 (1983).

[6] B.I. Halperin, Helv. Phys. Acta **56**, 75 (1983).

[7] A. H. MacDonald, Phys. Rev. B **37**, 4792 (1988).

[8] J. D. Nauda and Leonid P. Pryadko and S. L. Sondhi, Nuclear Physics B **594**, 713 (2001).

[9] X. Qiu, R. Joynt, and A. H. MacDonald, Phys. Rev. B **42**, 1339 (1990).

[10] C. B. Hanna, J. C. Díaz-Vélez, and A. H. MacDonald, Phys. Rev. B **65**, 115323 (2002).

[11] M. S. Dresselhaus and G. Dresselhaus, Adv. Phys. **30**, 139 (1981).

[12] P. K. Lam and S. M. Girvin, Phys. Rev. B **30**, 473 (1984).

[13] S. W. De Leeuw, J. W. Perram, and E. R. Smith, Proc. R. Soc. Lond. A **373**, 27 (1980).

[14] C. B. Clark, Phys. Rev. **109**, 1133 (1958).

[15] K. Maki and X. Zotos, Phys. Rev. B **28**, 4349 (1983).